

PACS numbers: 42.55. Rz;42.55. Xi; 42.60. Jf; 42.60. Da
DOI: 10.1070/QE2009v039n05ABEH013967

Efficient emission at 1908 nm in a diode-pumped Tm : YLF laser

N.G. Zakharov, O.L. Antipov, A.P. Savikin, V.V. Sharkov, O.N. Eremeikin, Yu.N. Frolov, G.M. Mishchenko, S.D. Velikanov

***Abstract*. Emission parameters at 1908 nm in a longitudinally-diode-pumped Tm : YLF laser are studied. The laser parameters are optimised to obtain the maximal power of high-quality cw radiation. The output power of ~ 27 W is obtained at the slope efficiency of ~ 50 % and total optical pump conversion efficiency of ~ 41 %.**

Keywords: *Tm : YLF-laser crystal, diode pumping, cross-relaxation process, laser cavity, two-micron laser radiation, lasing efficiency*.

1. Introduction

Highly-efficient and high-power solid-state lasers generating radiation beams in a long-wavelength part of the near-IR range (at the wavelength $\lambda > 1.4$ μm) are widely used in modern industrial technologies, remote atmospheric probing, medicine, military applications, and other fields [1 – 3]. The lasers on crystals doped with Tm^{3+} ions are capable of efficiently generating radiation at $\lambda = 1.9 - 2$ μm. Advantages of these lasers are determined by the properties of Tm^{3+} ions, which have a strong and wide absorption band near 800 nm, which is ideal for pumping by high-power laser diodes. These ions also possess cross-relaxation transitions, which provide appearance of two ions at the higher laser level per each quantum of the absorbed pump power [4, 5].

In recent years, lasers on crystals with Tm have been investigated in many research groups [6 – 15]. One of the most promising is a Tm : YLF crystal due to a strong natural birefringence (which provides a linear polarisation of generation), negative temperature coefficient of the refractive index (which weakens the total thermal lens of the active element compensated by a positive lens at the face ends and by the electron effect), wide luminescence band, which, in particular, well overlaps the absorption band of the Ho : YAG crystal [10, 11]. Tm : YLF lasers exhibit the possibility of generating high-power radiation in high-quality beams at a high efficiency of end or side diode pumping [10 – 13].

This paper is devoted to the study of the generation characteristics of an end-diode-pumped Tm : YLF laser and to the optimisation of its parameters aimed at increasing the cw output power at the high efficiency of pum radiation conversion.

2. Optical properties of the Tm : YLF crystal

Tm : YLF active elements used in our experiments were grown by the Bridgman – Stockbarger method (the atomic concentration C_{Tm} of Tm^{3+} atoms was 3 % and 3.5 %), cut in the form of a cylinder perpendicular to the crystal axis and had AR coated end faces at the pump and generation wavelengths of $\lambda_p = 793$ nm and $\lambda_g = 1908$ nm, respectively. The measured absorption spectrum of the Tm : YLF crystal showed strong absorption for both polarised and non-polarised radiation at the diode-array wavelength of ~ 800 nm (see Fig. 1).

The Tm : YLF crystal has a relatively low ($\sigma \approx 3 \times 10^{-21}$ cm^2) gain cross section at 1908 nm [10] and a high generation threshold due to the quasi-three-level scheme of generation. Hence, the efficient operation of the laser requires a high pump intensity. Actually, the permissible

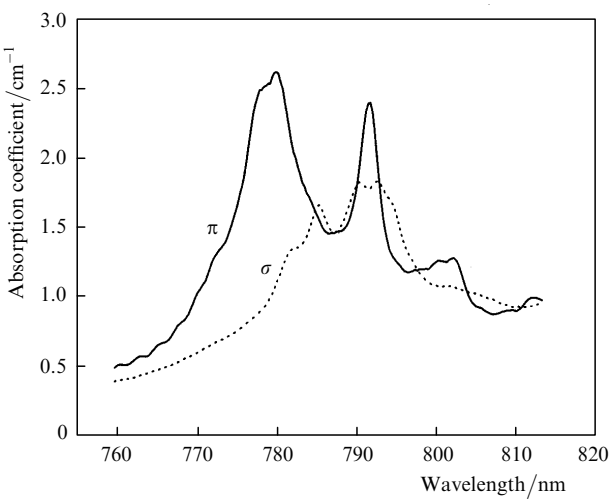

Figure 1. Absorption spectrum for the π- and σ-polarisations of the Tm : YLF crystal with the atomic concentration of Tm^{3+} ions $C_{Tm} = 3$ % measured with an MDR2 monochromator with the resolution of 0.5 nm.

N.G. Zakharov, O.L. Antipov, A.P. Savikin, V.V. Sharkov, O.N. Eremeikin Institute of Applied Physics, Russian Academy of Sciences, ul. Ul'yanova 46, 603950 Nizhnii Novgorod, Russia; e-mail: antipov@appl.sci-nnov.ru;
Yu.N. Frolov, G.M. Mishchenko, S.D. Velikanov Russian Federal Nuclear Center 'All-Russian Scientific Research Institute of Experimental Physics', prosp. Mira 37, 607190 Sarov, Nizhnii Novgorod region, Russia

Received 15 September 2008; revision received 21 October 2008
Kvantovaya Elektronika **39** (5) 410 – 414 (2009)
Translated by N.A. Raspopov

pump intensity is limited by the breakdown threshold of the laser crystal due to thermomechanical stresses inherent in it (the threshold pump power converted to heat per unit length of the Tm : YLF element is ~ 13 W cm^{-1}) [11].

The high conversion efficiency of pump radiation into generation radiation at $\lambda = 1.9$ μm (large quantum yield) is achieved in the Tm : YLF crystal mainly due to cross-relaxation transitions, which are caused by the interaction between Tm^{3+} ions. In the general case, the upper $^3F_4$ level of the laser transition in crystals with Tm^{3+} can be populated due to both the dipole–dipole ion interaction (which provides the cross-relaxation transitions $^3H_4 \rightarrow {}^3F_4$ and $^3H_6 \rightarrow {}^3F_4$), and intracentre decay (see Fig. 2). However, the probability of the cross-relaxation process is much greater than that of the radiation transition and radiationless relaxation [14–17]. This is expressed in the fact that the quantum yield η for the laser $^3F_4 \rightarrow {}^3H_6$ transition (upon pumping from the $^3H_6$ level to $^3H_4$ level) is close to two, and is equal to ~ 1.84 for $C_{Tm} = 3$ % [11]. On the other hand, the fact that $\eta < 2$, is explained by the energy deficiency for the cross-relaxation transition and luminescence branching from the $^3F_4$ level [6, 11, 14]. The excitation energy is also lost due to the absorption from the excited state to higher levels (for example, in the $^3H_5 \rightarrow {}^1G_4$ transition) or due to up-conversion (during the interaction of two excited Tm^{+3} ions) [11]. The luminescence of the Tm : YLF crystal observed in our experiments in the visible spectral range that corresponds, for example, to the $^1G_4 \rightarrow {}^3H_6$ transition also indicates that high levels are populated.

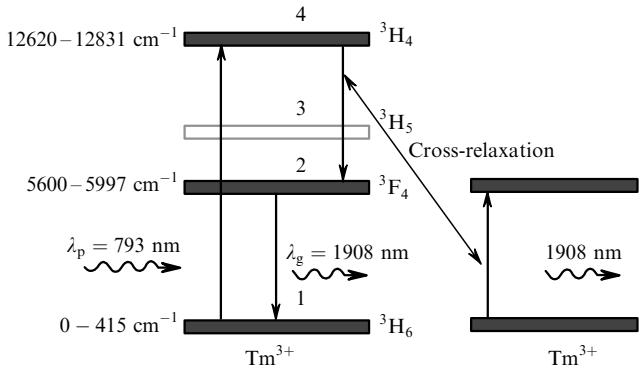

Figure 2. Diagram of laser levels for the Tm : YLF crystal.

3. Experimental

In the experiments, the active element from the Tm : YLF crystal was oriented so that the dichroic mirrors would introduce the lowest losses for the σ-polarisation at $\lambda_g = 1908$ nm. The U-shaped turning cavity was formed by four mirrors: a plane mirror M1 with a high reflection coefficient ($R = 99$ %) at $\lambda_g = 1908$ nm, the dichroic mirrors M2 with $R > 99$ % for vertical polarisation, and $R \sim 96$ % for horizontal polarisation at $\lambda_g = 1908$ nm and a high transmission for pump radiation at $\lambda_p = 793$ nm, as well as the output spherical mirror M3 (see Fig. 3).

The Tm : YLF crystal was pumped by two cw diode arrays with a fibre pigtail (the core diameter is 800 nm, the numerical aperture is ~ 0.13), which generated non-polarised radiation at the wavelength $\lambda_p = 793$ nm with the

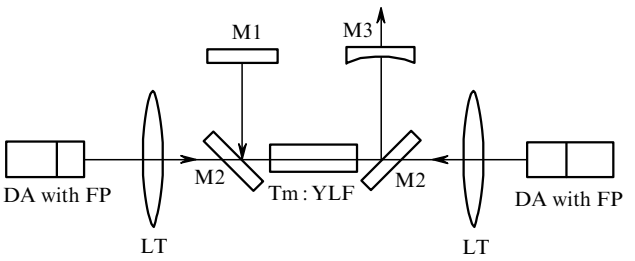

Figure 3. Scheme of the experimental setup: DA with FP is the diode array with a fibre pigtail; LT are two-lens telescopes with identical parameters; M1 is a highly reflecting mirror; M2 are dichroic mirrors; M3 is an output mirror.

power of up to 40 W. The laser diode wavelength was tuned and stabilised by a cooling system on Peltier elements with the electronic control of the temperature. The output beam of the diode arrays was focused by a telescope consisting of two spherical lenses into the Tm : YLF crystal through a dichroic mirror. In the experiments, we used the active elements of lengths $L = 10$, 14.5, and 16.5 mm, of diameter 3 mm, and concentrations $C_{Tm} = 3$ % and 3.5 %.

The element from Tm : YLF with $L = 10$ mm and $C_{Tm} = 3$ %. A cylindrical element from the Tm : YLF crystal of length 10 mm and diameter 3 mm was mounted on the heatsink, whose temperature was maintained constant (about 15 °C). The output mirror with the curvature radius $R_c = 200$ mm had a reflection coefficient $K = 83$ %. The cavity length varied from 8 to 15 cm. Calculations of the fundamental TEM_{00} mode showed that at the parameters L_{cav} and R_c given above the diameter of the fundamental cavity mode in the crystal does not exceed 600 μm (with the allowance made for a weak negative thermal lens having a focus length longer than 12 cm, which is induced in the crystal by intense pumping). Radiation from the two diode arrays was focused by two double-lens Kepler telescopes, which formed the pump zones with the diameters from 700 to 900 μm in the laser crystal (see Fig. 4). The focus distances of the lenses forming the telescopes could be varied. The pump beam diameter in the focal waist inside the active element was preliminarily

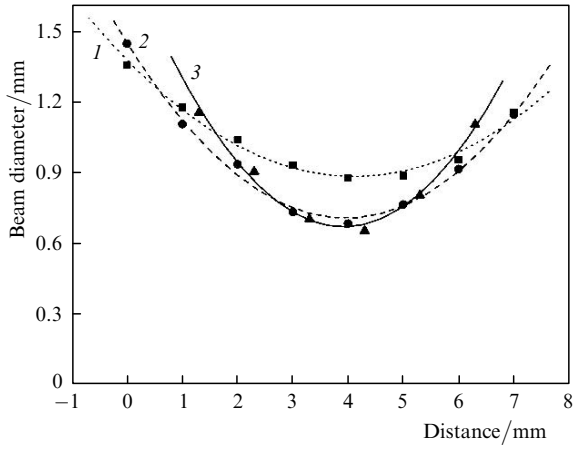

Figure 4. Dependences of the pump beam diameter on the distance to the focus for telescope 1 comprising similar lenses with the focal lengths $f = 5$ cm (*1*); for telescope 2 comprising lenses with $f = 5$ and 3.5 cm (*2*); and for telescope 3 comprising lenses with $f = 5$ and 3 cm (*3*).

measured in air (with the help of a USB-camera and LabVIEW and Vision software) in two ways: by reducing the intensity by a factor of e^2 and by determining the domain corresponding to 90 % of the total power.

The experiments were performed in turn with each of the pump telescopes. The greatest power of laser generation ($\sim$ 17 W at the slope efficiency of $\sim$ 30 %) was obtained with telescope 2 [see Fig. 5, curve (*1*)]. Employment of telescope 3 lowers the lasing threshold. In this case, the conversion efficiency of pump radiation into laser generation [curve (*2*)] is decreased. Telescope 1 increases the threshold at the constant slope efficiency of generation [curve (*3*)].

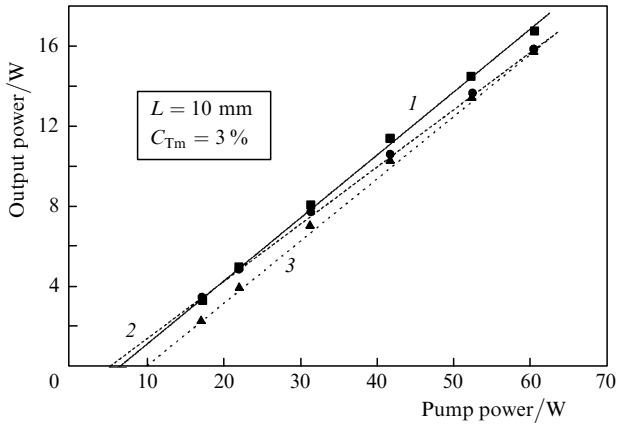

Figure 5. Dependences of the laser output power on the pump power in the scheme with telescope 2 (*1*), scheme with telescope 3 (*2*), and scheme with telescope 1 (*3*).

The element from Tm : YLF with L = 14.5 mm and C_{Tm} = 3 %. The gain domain inside the active element is formed by using lens telescopes 1 and 2, which convert the pump beam from diode arrays. By using the output mirror with R_c = 200 mm and K = 83 % in the $\sim$ 11-cm-long cavity, the greatest output power was obtained with telescope 1 [see Fig. 6, curve (*1*)]. In this case, a greater slope efficiency of generation was obtained ($\sim$ 49 %) due to the more extended caustic of the pump beam. Using telescope 2, the maximal slope efficiency was 45 %.

For obtaining a maximum power and increasing the efficiency of the laser system, the reflection coefficient of the output mirror R was optimised. Comparison of the laser power as a function of the pump power for two mirrors with $R \sim 83$ % and ~ 89 % [see Fig. 6, curves (*1*) and (*3*)] shows that the use of the mirror with a lower Q factor ($R \sim 83$ %) not only increases the laser threshold but also results in a greater slope efficiency.

Elements from Tm : YLF with various L and C_{Tm}. Experiments were also carried out using elements from Tm : YLF with C_{Tm} = 3 % and the lengths of 14.5 mm (element 1) and 16.5 mm (element 2). Similarly to the previous cases, the active element was mounted on a heatsink whose temperature was maintained constant (about 15 °C). The pump beam was formed by telescope 1. The reflection coefficient of the output mirror was 83 %.

The best results (with respect to the output power) were obtained with active element 1 [see Fig. 7, curve (*1*)]. The maximal slope efficiency of 52 % (the measurement error

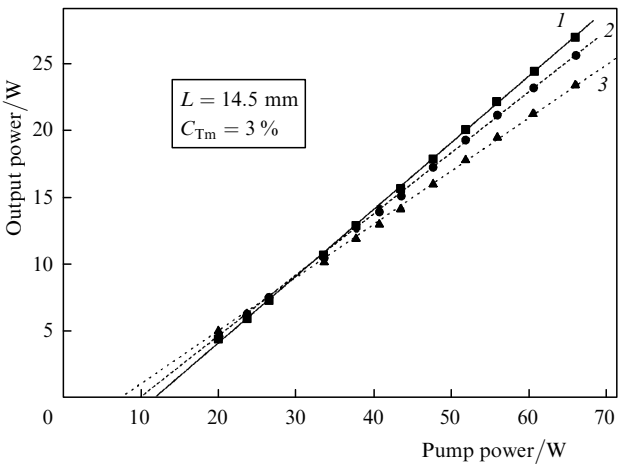

Figure 6. Dependences of the laser output power on the pump power in the scheme with telescope 1 and the mirror with $R \sim 83$ % (*1*), scheme with telescope 2 and the mirror with $R \sim 83$ % (*2*), and scheme with telescope 1 and the mirror with $R \sim 89$ % (*3*).

was no greater than 0.5 %) was obtained with element 3 [curve (*3*)], which was by 2 % greater than that obtained with elements 1 or 2. The better slope efficiency of generation can be explained by a higher quantum efficiency of the cross-relaxation population of the working $^3H_4$ level of the Tm^{3+} ion at a greater concentration of activator ions [11]. Nevertheless, the generation threshold of the laser with active elements 2 and 3 was $\sim$ 14 W, which is greater than that with element 1. Thus, the total power conversion efficiency of the pump beam incident on the crystal into the laser beam power was maximal with active element 1 and amounted to $\sim$ 41 %.

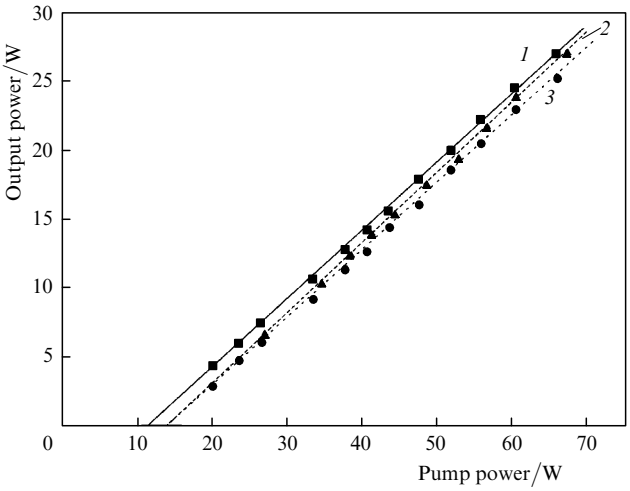

Figure 7. Dependences of the laser output power on the pump power in the scheme with element 1 (C_{Tm} = 3 %, L = 14.5 mm) (*1*), element 2 (C_{Tm} = 3 %, L = 16.5 mm) (*2*), and element 3 (C_{Tm} = 3.5 %, L = 14.5 mm) (*3*).

Spectrum and spatial structure of the laser beam. The laser emission spectrum was studied with an MDR2 optical monochromator and a photoresistor on the KPT structure with a response time of $\sim 10^{-8}$ s. The spectral resolution of the monochromator was $\sim$ 0.5 nm. The chosen orientation of the Tm : YLF crystal and the polarisation selectivity of

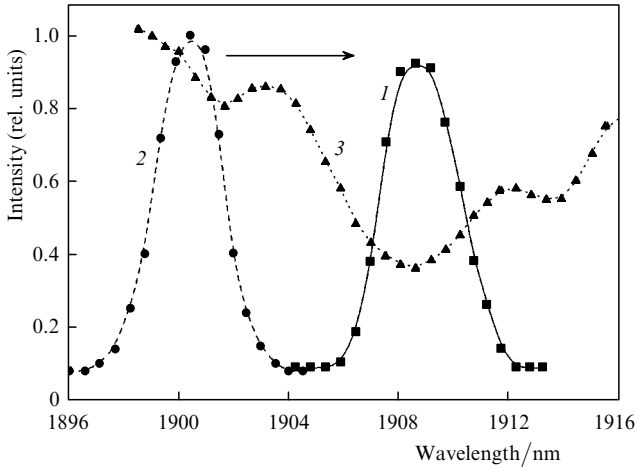

Figure 8. Emission spectrum of the Tm : YLF laser at the output power of 25 W.

the cavity mirrors provided stationary σ-polarised generation at ~ 1908 nm (see Fig. 8). The measured emission spectrum approximated by a continuous curve had a maximum at $\lambda = 1908.5 - 1908.8$ nm. One can see that the laser line well agrees with one of the absorption maxima in the Ho : YAG crystal [see Fig. 8, curve (*3*)].

Note that the emission spectrum first arises at the wavelength of ~ 1900 nm [Fig. 8, curve (*2*)] and then it moves to $\lambda_g \sim 1908$ nm [curve (*1*)]. This can be explained by splitting of the lower level of the laser working transition in the active element to nine Stark sublevels. The generation first arises at a short-wavelength transition which has the greatest gain cross section. In the process of generation, the temperature of the active element rises and the population distribution at lower sublevels changes, which results in a reduction of both the inversion population and gain at the short-wavelength transition as compared to the long-wavelength one. The rate of the spectrum motion from 1900 nm to 1908 nm depends on the temperature and diameter of the crystal as well as on the pump power. At the crystal temperature of 14 °C, diameter of 5 mm, and pump power of 50 W, the characteristic transient period for establishing the stationary spectrum (at 1908 nm) was ~ 0.3 s.

Rotation of the active element around its axis at the same cavity parameters resulted in generation at ~ 1880 nm, which corresponds to the maximum of the π-polarised luminescence line in the Tm : YLF crystal.

The spatial structure of Tm : YLF-laser beam studied with the IR camera is presented in Fig. 9. The quality parameter M^2, which characterises the ratio of the laser beam divergence to the diffraction divergence of the Gaussian beam, was determined according to the ISO standard [18]. It was found that at the laser power of ~ 25 W (mirror with $R = 83\,\%$), we have $M^2 \approx 2.5$, which proves that even at the maximum power the laser beam is close to a single-mode one.

Generation dynamics of the Tm : YLF laser. Time characteristics of generation were measured with a photoresistor based on the KPT structure with the detection ability at room temperature of $(3 - 10) \times 10^{10}$ cm Hz$^{1/2}$ W^{-1}. The signal was fed to a LeCroy 62Xi oscilloscope with the bandwidth of 600 MHz. In all the measurements a spiking regime of generation was observed with the characteristic pulse duration of 2–5 μs and the period of 3–10 μs

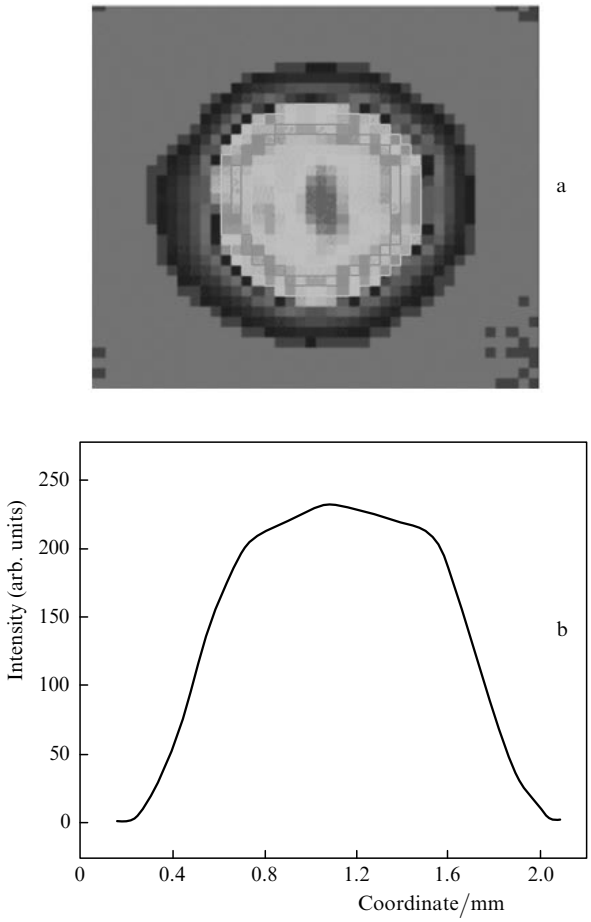

Figure 9. Photograph of the Tm : YLF-laser beam obtained with a 'Pyrocam' camera (a) and the transverse intensity distribution of the beam (b).

reducing at a higher laser power (see Fig. 10). The non-dumped pulses in a Tm : YLF laser were earlier explained by the saturated absorption of the water vapour at the laser wavelength [13]. However, in our experiment the reduction of air moisture from 30 % to $\sim 5\,\%$ (by filling a specially constructed cell with argon) did not affect the spike

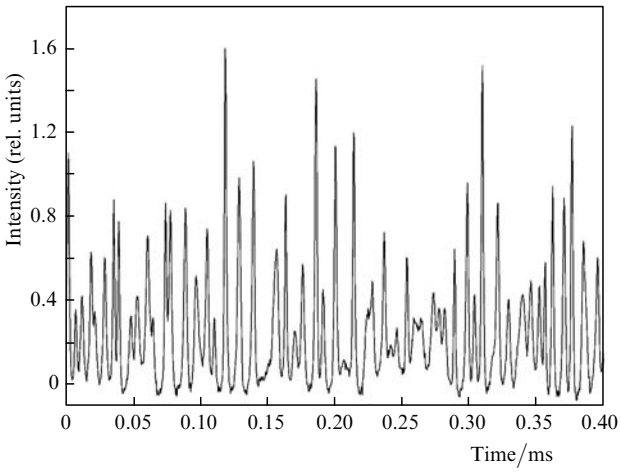

Figure 10. Dynamics of the output power of the Tm : YLF laser in the scheme with the element of length $L = 14.5$ mm and $C_{Tm} = 3\,\%$ at the output power of 25 W.

structure. It is more likely that the spike structure is related to the specific features of relaxation oscillations in a solid-state laser on a crystal with the quasi-three-level scheme of generation and a long lifetime of the metastable level in the presence of cross-relaxation and up-conversion processes [19, 20].

4. Conclusions

Diode-pumped Tm : YLF lasers have been studied. The pump scheme, crystal length, and cavity configuration have been optimised. The cw power of ~ 27W has been obtained at the slope efficiency of 50 % and the beam quality parameter $M^2 \sim 2.5$. The emission spectrum of the stationary laser with no particular selection has been observed in the range of 1908 nm and had the width of ~ 4 nm. The high generation efficiency of the laser and compactness of its optical scheme are promising for it employment in medicine, material treatment, remote atmosphere monitoring, and other scientific and technologicqal applications.

References

1. Tag R., Steakley B.C., Hawley J.G., et al. *Appl. Opt*., **35**, 7117 (1996).
2. Sudrsh V., Piper J.A. *IEEE J. Quantum Electon*., **36**, 879 (2000).
3. Theisen D., Ott V., Bernd H.W., et al. *Proc. SPIE Int. Soc. Opt. Eng*, **5142**, 96 (2003).
4. Noginov M.A., Prokhorov A.M., Sarkisyan G.K., Smirnov V.A., Shcherbakov I.A. *Kvantovaya Elektron*., **18** (9), 1042 (1991) [*Sov. J. Quantum Electron*., **21** (9), 945 (1991)].
5. Stoneman R.C., Esterovitz L. *IEEE J. Sel. Top. Quantum Electron*., **18**, 78 (1995).
6. Borodin N.I., Kryukov P.V., Popov A.V., Ushakov S.N., Shestakov A.V. *Kvantovaya Elektron*., **35** (6), 511 (2005) [*Quantum Electron*., **35** (6), 511 (2005)].
7. Bagayev S.N., Vatnik S.M., Maiorov A.P., Pavlyuk A.A., Plakushchev D.V. *Kvantovaya Elektron*., **30** (4), 310 (2000) [*Quantum Electron*., **30** (4), 310 (2000)].
8. Mateos X., Petrov V., Liu J., Pujol M.C., et al. *IEEE J. Quantum Electron*., **42** (10), 1008 (2006).
9. *Novel Materials and Laser Sources*, in *Techn. Dig. 2nd EPS-QEOD Europhoton Conf. on Solid-State and Fiber Coherent Light Sources* (Pisa, Italy, 2006).
10. Budni P.A., Lemos M.L., Mosto J.R., Chicklis E.P. *J. Sel. Top. Quantum Electron*., **6**, 629 (2000).
11. So S., Mackenzie J.I., Shepherd D.P., Clarkson W.A., Betterton J.G., Gorton E.K. *Appl. Phys. B*, **84**, 389 (2006).
12. Dergachev A., Wall K., Moulton P.F. *OSA TOPS*, *Adv. Sol.-State Lasers*, **68**, 343 (2002).
13. Schellhorn M., in *Techn. Dig. Top. Meet. '2007 Advanced Solid-State Photonics'* (Washington DC: OSA, 2008) Paper WE33.
14. Walsh B.M., Barnes N.P., Di Bartolo B. *J. Appl. Phys*., **83** (5), 2772 (1998).
15. Ryba-Romanowski W., Golab S., Sokolska I., Dominiak-Dzik G., Zawadzka J., Berkowski M., Fink-Finowicki J., Baba M. *Appl. Phys. B*, **68**, 199 (1999).
16. Sveshnikova E.B., Stroganov A.A., Timofeev N.T. *Opt. Spektros*., **175**, 4 (1986).
17. Miyakawa T., Dexter D.L. *Phys. Rev. B*, **1** (7), 2961 (1970).
18. *Optics and Optical Instruments –Test Methods for Laser Beam Parameters: Beam Width, Divergence Angle and Beam Propagation Factor* (ISO/DIS 11 146:1999, 1999).
19. Cerny P., Valentine G.J., Burns D. *Electron. Lett*., **40** (17), 1061 (2004).
20. Louchev O.A., Urata Y., Wada S. *Opt. Express*, **15** (7), 3940 (2007).